Food Research International 43 (2010) 2057–2067

Contents lists available at ScienceDirect

Food Research International

journal homepage: www.elsevier.com/locate/foodres

Effect of TAG composition on the crystallization behaviour of model fat blends with the same saturated fat content

Jeroen Vereecken [a,*], Veerle De Graef [a], Kevin W. Smith [b], Johan Wouters [c], Koen Dewettinck [a]

[a] Department of Food Safety and Food Quality, Laboratory of Food Technology and Engineering, Faculty of Bioscience Engineering, Ghent University, Coupure Links 653, 9000 Gent, Belgium
[b] Consultant to Loders Croklaan, Fat Science Consulting Ltd., 16 Arundel Drive, Bedford, Bedfordshire, MK41 8HP, United Kingdom
[c] Laboratoire de Chimie Biologique Structurale, Facultes Universitaires Notre-Dame de la Paix, Namur, Belgium

ARTICLE INFO

Article history:
Received 20 January 2010
Accepted 17 June 2010

Keywords:
Triacylglycerols
Trisaturated
Symmetry
Stop-and-return DSC
Polymorphism

ABSTRACT

In this study, the crystallization and polymorphic properties of eight fat blends with the same saturated fat content (50%) but with a varying TAG composition were investigated using DSC and X-ray diffraction. Blends were either palmitic (P) or stearic (S) based, and were all diluted with high oleic sunflower oil to obtain the same level of saturated fatty acids. Three different effects were investigated, namely the effect of chain length, the effect of trisaturated TAG and the effect of symmetry. The DSC results suggested that PPP, present in the palmitic based blends, seeded the crystallization process better than did SSS in the stearic based blends. Stop-and-return DSC revealed a two-step crystallization for almost all the blends at 15 °C, 20 °C and 25 °C. This behaviour was further elucidated by WAXD-analysis of the blends, showing an initial crystallization into an unstable polymorph followed by polymorphic transformation during crystallization.

1. Introduction

TAG crystallization forms the basis for the development of a fat crystal network that is directly related to the macroscopic properties of the end products such as spreadability, hardness and mouth feel. As such, the TAG composition of a fat system is of primary importance for the consumers' perception of the end products (Narine & Marangoni, 1999; Marangoni, 2002; Sato, 2001). Small changes in the TAG composition can have a big impact on the crystallization and polymorphic properties of the fats, as demonstrated in the important reviews of Timms (1984), Sato (2001) and Himawan, Starov, and Stapley (2006). The application of fat modification to create more 'healthy' fats has thus an enormous impact on the crystallization, polymorphism and further structural development of the fat products, which is already described in a broad range of studies. Modification techniques include hydrogenation, fractionation, interesterification, and blending.

Hydrogenation invokes an increase in the melting point of the fats and thus also a change in the crystallization properties, due to a change from unsaturated to saturated fatty acids. In the past, this technique was frequently used and better known as 'fat hardening' in the margarine industry. Partially hydrogenated fats and oils, which are frequently used in shortenings and confectionery products, are a major source of trans fatty acids. However, due to upcoming health recommendations concerning the maximum level of trans and saturated fatty acids in food oils and fats, the food industry is searching for strategies to change the TAG composition of the food oils and fats to reduce these fatty acids to appropriate levels (List, 2004).

The easiest fat modification technique is blending. Several studies investigate blends consisting of a high melting component diluted in a liquid vegetable oil, for example as an alternative of trans and saturated fatty acids (e.g. Danthine & Deroanne, 2003; Toro-Vazquez, Briceno-Montelongo, Dibildox-Alvarado, Charo-Alonso, & Reyes-Hernandez, 2000).

Another method to combine the different properties of fats is the use of enzymatic or chemical interesterification, leading to completely different results depending on the experimental set-up. To give an example, Zhang, Smith, and Adler-Nissen (2004) investigated the effect of degree of enzymatic interesterification on the physical properties of margarine fats, revealing the occurrence of a higher amount of β′ crystals for a higher degree of interesterification. On the other hand, Karabulut, Turan, and Ergin (2004) investigated the effects of chemical interesterification on solid fat content and slip melting point of fat/oil blends. From this study it was clear that softer products were obtained after interesterification.

A last important modification technique is fractionation, which is especially used in the palm oil and butter (milk fat) industry (Deffense, 1985). The crystallization properties of palm oil and its fractions depend largely on the fractionation conditions. (Zaliha, Chong, Cheow, Norizzah, & Kellens, 2004). Also, the polymorphism is very important during the fractionation of palm oil, with the occurrence of both β′ and β polymorphs (Braipson-Danthine, & Gibon, 2007).

The above-mentioned studies especially focus on the crystallization and polymorphic properties. On the other hand, different studies

* Corresponding author. Tel.: +32 9 264 61 68; fax: +32 9 264 62 18.
E-mail address: Jeroen.Vereecken@UGent.be (J. Vereecken).

0963-9969/$ – see front matter © 2010 Elsevier Ltd. All rights reserved.
doi:10.1016/j.foodres.2010.06.008

go back to the molecular level and describe the crystallization and phase behaviour of pure triacylglycerols (Timms, 1984; Himawan et al., 2006). Each TAG is characterized by a specific polymorphic behaviour and corresponding melting properties. Small changes in the structure of the TAG molecule will have a big impact on their properties, for example, POP (P = palmitic and O = oleic) forms a β stable triple chain length structure, while PPO is characterized by a β′ stable triple chain length structure. The 1:1 compound of POP and PPO is characterized by a β stable double chain length structure (Minato, Ueno, Smith, Amemiya, & Sato, 1997). Also SOS (S = stearic) and SSO are characterized by a comparable behaviour (Takeuchi, Ueno, & Sato, 2002). Systems with symmetric TAG (e.g. POP, SOS and POS) and trisaturated TAG (e.g. PPP and SSS) have also been investigated, with differential scanning calorimetry (DSC) and X-ray diffraction (XRD) being the most important measurement techniques. For example, Minato et al. (1996) described the phase behaviour of PPP–POP mixtures. Under certain conditions, some mixtures of these two TAG form solid solutions governed by a monotectic phase behaviour. Wesdorp (1990) has also reported a number of phase diagrams, including SSS–OOO and PPP–OOO. These show that OOO, up to a certain degree, is incorporated into the solid phase, so it does not act as a pure 'solvent' for the higher melting TAG. In fact, the same behaviour is valid for PPP (high melting component) and POP (low melting component) (Minato et al., 1996; Smith, Cain, & Talbot, 2005).

Clearly, two types of studies can be discerned, namely applied studies and fundamental studies. On the one hand, the applied studies focus on the physical behaviour of natural oils and fats and their application in the industry. They rarely focus on TAG composition and molecular interactions and they have not been designed specifically to study blends with the same level of saturated fat and a specific TAG composition. On the other hand, the fundamental studies, investigating mixtures of pure TAG, are usually too far removed from industrial applications. Therefore, the objective of this research was focused between these two types of studies by investigating blends of natural fats and oils from a TAG point of view. This kind of research has already been carried out by the authors' group (Vereecken, Foubert, Smith, & Dewettinck, 2009), using fat blends all having a saturated fat content of 30%.

The aim of the present study was to investigate blends all having a saturated fat content of 50%, which is closer to that of fats used in confectionery products (e.g. coatings) (Timms, 2003). The fat blends were constructed in such a way that three different effects of TAG composition could be evaluated: the effect of chain length by using palmitic based and stearic based fats, the effect of trisaturated TAG by varying the amount of PPP and SSS and the effect of symmetry by varying the amount of symmetric and asymmetric TAG. As such, eight blends were constructed and the crystallization and polymorphic behaviour were compared using differential scanning calorimetry and X-ray diffraction.

2. Materials and methods

2.1. Samples

Palm-mid fraction (PMF, a POP source), interesterified palm-mid fraction (iPMF, a PPO source), shea stearin (SHs, an SOS source), interesterified shea stearin (iSHs an SSO source), palm stearin (POs, a PPP source), fully hydrogenated soybean oil (FHSBO, an SSS source) and high oleic sunflower oil (HOSF) were used as starting oils for the blends and were provided by Loders Croklaan (Wormerveer, The Netherlands).

2.2. Fatty acid composition

Fatty Acid Methyl Esters (FAME) were produced by dissolving 1 drop (10–20 mg) of sample in 9 mL hexane and reacting with 1 mL 2 N KOH/methanol reagent. The mixture was shaken for 30 s at room temperature and then allowed to settle. Approximately 1.5 mL of the hexane layer was carefully decanted into a GC vial. High resolution FAME GC was carried out on an Interscience Thermofocus GC with a RTX-2330 column (cyanopropyl polysiloxane, 60 m length, 0.25 mm internal diameter, and 0.2 μm layer thickness). Hydrogen was used as carrier gas. 1.0 μL of sample solution was injected via a split/splitless injector (split ratio: 20:1) using an autosampler. The oven temperature was programmed starting at 50 °C for 8 min, from 50 to 182 °C at 5 °C/min, holding at 182 °C for 20 min, from 182 to 200 °C at 5 °C/min and holding at 200 °C for 5 min. Detection was via FID set to 250 °C. The results were based on single measurements since the intended compositional differences were much larger than the likely errors.

2.3. TAG composition

Separation of TAG components, including positional isomers, was achieved by high performance liquid chromatography on silver loaded silica, based upon a modification of the procedure originally described by Jeffrey (1991). A 3-micron Nucleosil 100 silica was impregnated with a 10% silver nitrate and packed into a 150 mm × 4.6 mm steel column. HPLC was performed using a Varian 9010 ternary pumping system (Varian Inc, UK) in conjunction with a Gilson 231 autosampler (Anachem, UK). HPLC peak detection was achieved with a Polymer Labs 2100 light scattering detector (Varian Polymer Labs, Varian Inc, UK). TAG separation was achieved using the same methodology as in the previous work of the author's group (Vereecken, Foubert, Smith, & Dewettinck, 2010). As for FAME analysis, single determinations were made.

2.4. Making of the blends

The blends were made based on the fatty acid and TAG composition of the starting oils (see first part in the 'Results and Discussion' sections). Each starting oil was placed in an oven at 90 °C till completely liquid. Then the appropriate masses for the blends were weighed into a glass beaker and the oils were mixed with a magnetic stirrer equipped with a heating block to ensure that no fat crystallized during the mixing process. When the oils were completely mixed, the blend was poured into a plastic cup for further analysis.

2.5. Isothermal crystallization curve using DSC

The isothermal crystallization curves were obtained with a TA Q1000 DSC (TA Instruments, New Castle, Delaware) with a Refrigerated Cooling System. The DSC was calibrated with indium (TA Instruments, New Castle, Delaware), azobenzene (Sigma-Aldrich, Bornem, Belgium) and undecane (Acros Organics, Geel, Belgium) before analyses. Nitrogen was used to purge the system. Fat (5–15 mg) was hermetically sealed in aluminum pans using sample preparation procedure B as described by Foubert, Vanrolleghem, and Dewettinck (2003) and an empty pan was used as a reference. The time-temperature program applied was as follows: holding at 80 °C for 15 min to ensure a completely liquid state, cooling at 25 °C/min to the isothermal crystallization temperature (15 °C, 20 or 25 °C, and ± 0.05 °C), holding for 180 min at this temperature. The high cooling rate was applied to limit the amount of fat crystallizing during the cooling. Results were presented using the TA Universal Analysis 2000 software (TA instruments, New Castle, Delaware).

2.6. Isothermal crystallization kinetics using the DSC stop-and-return technique

Some samples already began to crystallize during the cooling process making it impossible to calculate the crystallization enthalpy of the isothermal period. Therefore, the samples were also analyzed

with DSC using the stop-and-return technique, which has been comprehensively described by Foubert, Fredrick, Vereecken, Sichien, and Dewettinck (2008), using crystallization temperatures of 15 °C, 20 °C and 25 °C. The data were fitted to the Foubert model, using SigmaPlot™ for Windows version 10.0 (SPSS Inc, Chicago, USA). Three kinetic model parameters were derived from the fitting, namely the induction time (min), the parameter K (min^{-1}) and the parameter a (J/g). The parameter K is related to the slope of the curves: a higher slope (which corresponds to a faster crystallization) results in a higher value for the parameter K. The parameter a gives the maximum value of the curve fitting after long isothermal times and is thus a measure of the equilibrium melting enthalpy at the end of the crystallization process (Foubert, 2003).

2.7. WAXD-analysis

The wide angle X-ray diffraction (WAXD) of the samples, to analyze the lateral packing (short spacings) of the different crystal polymorphs, was performed at the Laboratoire de Chimie de la Biologie Structurale, Facultés Universitaires de Notre-Dame de la Paix, Namur, Belgium.

The short spacings were measured on an X'pert Pro diffractometer (PANalytical, Almelo, The Netherlands) and an Anton Paar TTK-450 sample stage (Anton Paar Benelux, Sint-Martens-Latem, Belgium). An external water bath was used to apply the same time-temperature protocol as used in DSC. The diffractometer was equipped with a sealed Cu-X-ray tube, 0.04 rad primary and secondary Soller slits (size 2″) and a Ni-filter that produces a Cu Kα1 X-ray beam (λ = 1.541 Å). The sample was scanned from 15°2θ to 27.7°2θ, increasing with a step size of 0.008°2θ (0.04 s per step).

The WAXD-patterns obtained were smoothed with a Fourier transformation by the X'pert High Score software (PANalytical, Almelo, The Netherlands). Spreadsheets were generated of each scan with the diffraction intensity as function of the incident beam angle. The relationship between incident beam angle (θ) and short spacings (d) is given by Bragg's law (Eq. (1)):

$$d = \frac{n'\lambda}{2\sin\theta} \quad (1)$$

in which n' is the order of diffraction and λ is the wavelength (Å) used. 2D-plots of the obtained results were drawn in SigmaPlot™ for Windows version 10.0 (SPSS Inc, Chicago, USA).

3. Results

3.1. Blend composition

Based on the fatty acid and TAG composition of the starting oils (Table 1), eight blends were constructed to investigate the effect of trisaturated TAG, symmetry and chain length. The composition of these blends is shown in Table 2. From Table 1 it is clear that palm stearin (POs) and especially fully hydrogenated soybean oil (FHSBO) are highly saturated, as expected. These two oils were used as PPP source and SSS source, respectively, to investigate the effect of trisaturated TAG. Furthermore, the interesterified starting oils (iPMF and iSHs) do not only contain a high amount of the asymmetric TAG SatSatO, but also a high amount of trisaturated TAG (SatSatSat). Therefore, to investigate the effect of symmetry, extra trisaturated TAG were added to the symmetric starting oils (PMF and SHs). Finally, all blends were diluted with HOSF to obtain 50% SFA.

Blends PH and SH were prepared starting from the PPP source (palm stearin) and SSS source (hydrogenated soybean oil). Extra SHs was added to blend SH in order to have a SatSatSat/SatOSat ratio (Sat = saturated) similar to the PH blend (a low amount of disaturated TAG was present in palm stearin, see Table 1), and to allow comparison of blend PH with blend SH to see the different effects of PPP and SSS. Blends PM, iP, SM and iS were constructed in such a way that they contain almost the same level of trisaturated and disaturated TAG, so it is possible to compare the crystallization properties of these blends. Blends iP and iS do not have added PPP or SSS source, because the interesterified oils already contain a high amount of trisaturated TAG (see Table 1). Finally, blends PL and SL were made starting from PMF and SHs without the addition of extra PPP or SSS.

The TAG profiles of the resulting blends are presented in Table 3 and were calculated based on the TAG composition of the blend components presented in Table 1. As intended, the level of SatSatSat decreases from blend PH, over blend PM to blend PL and from blend SH, over blend SM to blend SL. This makes it possible to evaluate the effect of trisaturated TAG by comparing blend PH with blend PM and blend PL and by comparing blend SH with blend SM and blend SL.

Table 1
Fatty acid and triacylglycerol composition (%) of the initial oils with the amount of saturated fatty acids (SFA) in each oil (%).

Compound	POs	PMF	iPMF	FHSBO	SHs	iSHs	HOSF
Fatty acid							
C 16:0	80.59	57.75	57.65	9.82	4.49	3.35	3.82
C 18:0	5.48	6.09	5.86	86.54	58.08	58.99	3.00
C 18:1c	9.86	31.45	30.91	0.37	32.31	31.95	81.85
C 18:2n−6	2.03	2.95	2.69	0.00	3.17	2.66	8.92
SFA	87.89	65.36	64.92	99.60	64.34	63.77	8.03
TAG							
SatSatSat	77.2	4.2	28.3	99.9	1.2	27.7	0.0
SatOSat	12.4	77.6	13.4	0.1	83.7	13.5	0.4
OSatSat	2.1	6.9	26.9	0.0	1.0	27.0	0.0
SatLSat	1.6	6.2	1.3	0.0	7.6	1.2	0.1
SatSatL	0.2	0.5	2.7	0.0	0.0	2.5	0.0
SatOO	4	2.9	12.7	0.0	4.8	13.2	15.9
OSatO	0.1	0.1	6.4	0.0	0.0	6.6	0.0
SatOL/SatLO	1.1	0.6	3.8	0.0	0.4	3.6	1.3
OSatL	0.1	0.1	0.0	0.0	0.2	0.0	1.0
OOO	0.4	0.2	3.0	0.0	0.5	3.2	69.6
>3 d.b	0.9	0.7	1.2	0.0	0.6	1.2	11.8

SFA = saturated fatty acids, Sat = saturated, O = oleic acid, and L = linoleic acid.

Table 2
Oil composition (%) of the eight blends investigated.

Blend	Oils						
	POs	PMF	iPMF	FHSBO	SHs	iSHs	HOSF
PH	52.6						47.4
PM	29.2	32.6					38.3
PL		73.2					26.8
iP			73.8				26.2
SH				40.4	8.9		50.7
SM				22.6	37.8		39.6
SL					74.5		25.5
iS						75.3	24.7

Table 3
TAG profile (%) of the eight blends investigated.

TAG	PH	PM	PL	iP	SH	SM	SL	iS
SatSatSat	40.6	23.9	3.1	20.9	40.5	23.0	0.9	20.9
SatOSat	6.7	29.1	56.9	10.0	7.7	31.8	62.5	10.3
OSatSat	1.1	2.9	5.1	19.8	0.1	0.4	0.7	20.3
SatLSat	0.9	2.5	4.6	1.0	0.7	2.9	5.7	0.9
SatSatL	0.1	0.2	0.4	2.0	0.0	0.0	0.0	1.9
SatOO	9.6	8.2	6.4	13.6	8.5	8.1	7.6	13.9
OSatO	0.1	0.1	0.1	4.7	0.0	0.0	0.0	5.0
SatOL/SatLO	1.2	1.0	0.8	3.1	0.7	0.7	0.6	3.0
OSatL	0.5	0.4	0.3	0.3	0.5	0.5	0.4	0.2
OOO	33.2	26.8	18.8	20.5	35.3	27.8	18.1	19.6
>3 d.b	6.1	5.0	3.7	4.0	6.0	4.9	3.5	3.8

SFA = saturated fatty acids, Sat = saturated, O = oleic acid, and L = linoleic acid.

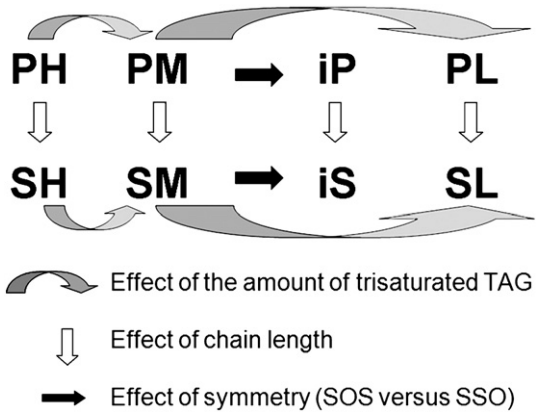

Fig. 1. General scheme of the research with an indication of the different investigated effects of TAG composition.

Furthermore, blend PM and iP contain almost the same level of trisaturated and disaturated TAG, enabling the assessment of the effect of symmetry by comparing these two blends. The same is valid for blend SM and iS. Finally, the effect of chain length can be investigated by comparing the palmitic based blends (PH, PM, PL and iP) with their stearic based alternative (SH, SM, SL and iS). Fig. 1 summarizes these comparisons.

3.2. DSC analyses

The isothermal crystallization of the investigated blends was evaluated by DSC measurements at three different crystallization temperatures, namely 15 °C, 20 °C and 25 °C. Fig. 2 illustrates the effect of trisaturated TAG at the three temperatures for the palmitic based (left side) and stearic based (right side) blends. Correspondingly, Fig. 3 shows the effect of symmetry for palmitic and stearic based blends. The effect of chain length is studied by comparing the palmitic based with the stearic based blends in both figures (see also Fig. 1). To gain more insight, the blends were also analyzed by the stop-and-return technique (Foubert et al., 2008), of which the results are shown in Fig. 4 (effect of trisaturated TAG) and 5 (effect of symmetry). The data points in these graphs were fitted using the Foubert (2003) model, indicated by the solid lines in Figs. 4 and 5. The derived model parameters are presented in Table 4. It was impossible to model the first crystallization step, because this step occurred partially during the non-isothermal cooling period and partially during the isothermal crystallization period. Therefore, it was only possible to properly model the second crystallization step of the blends.

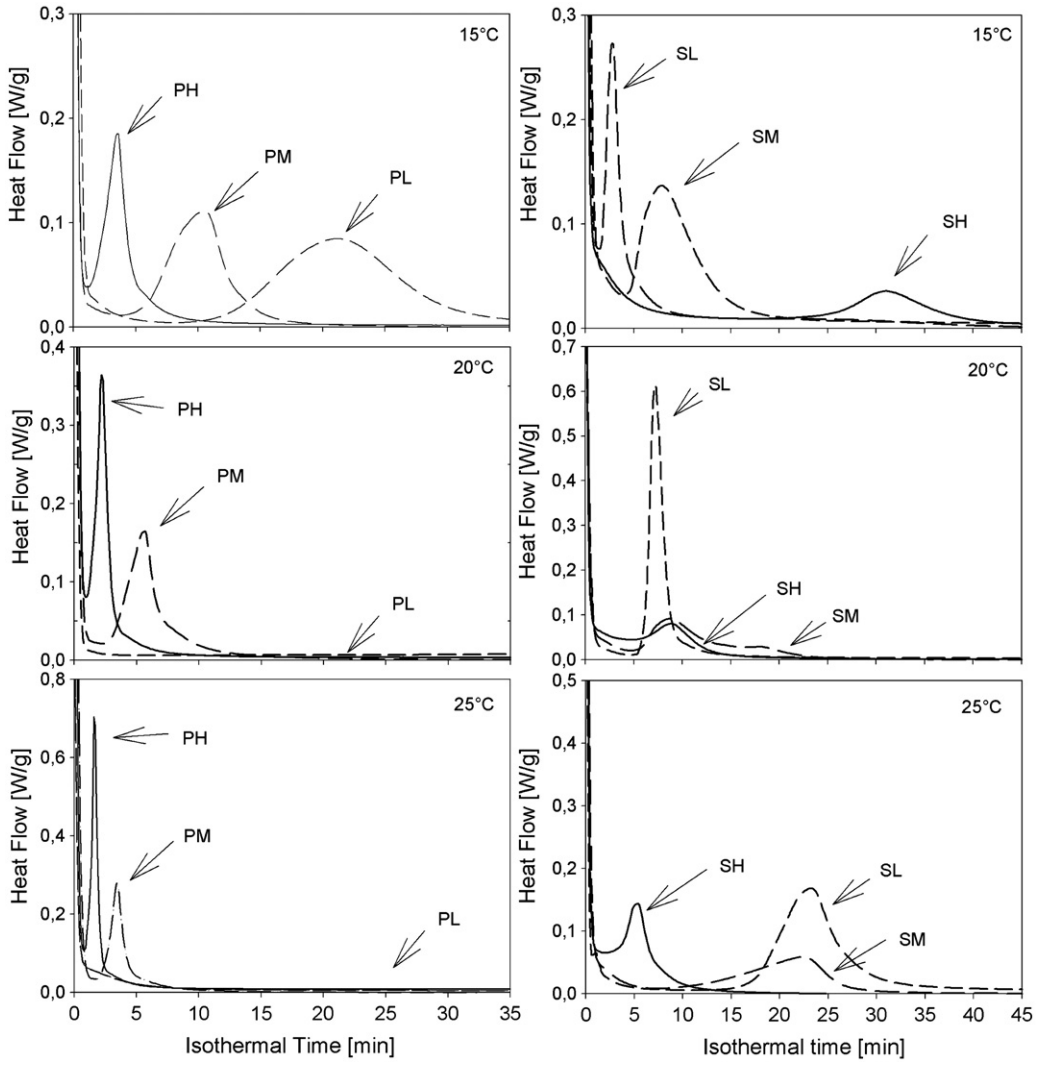

Fig. 2. Effect of trisaturated TAG on the isothermal DSC profiles at 15 °C, 20 °C and 25 °C. Left side: palmitic based blends and right side: stearic based blends.

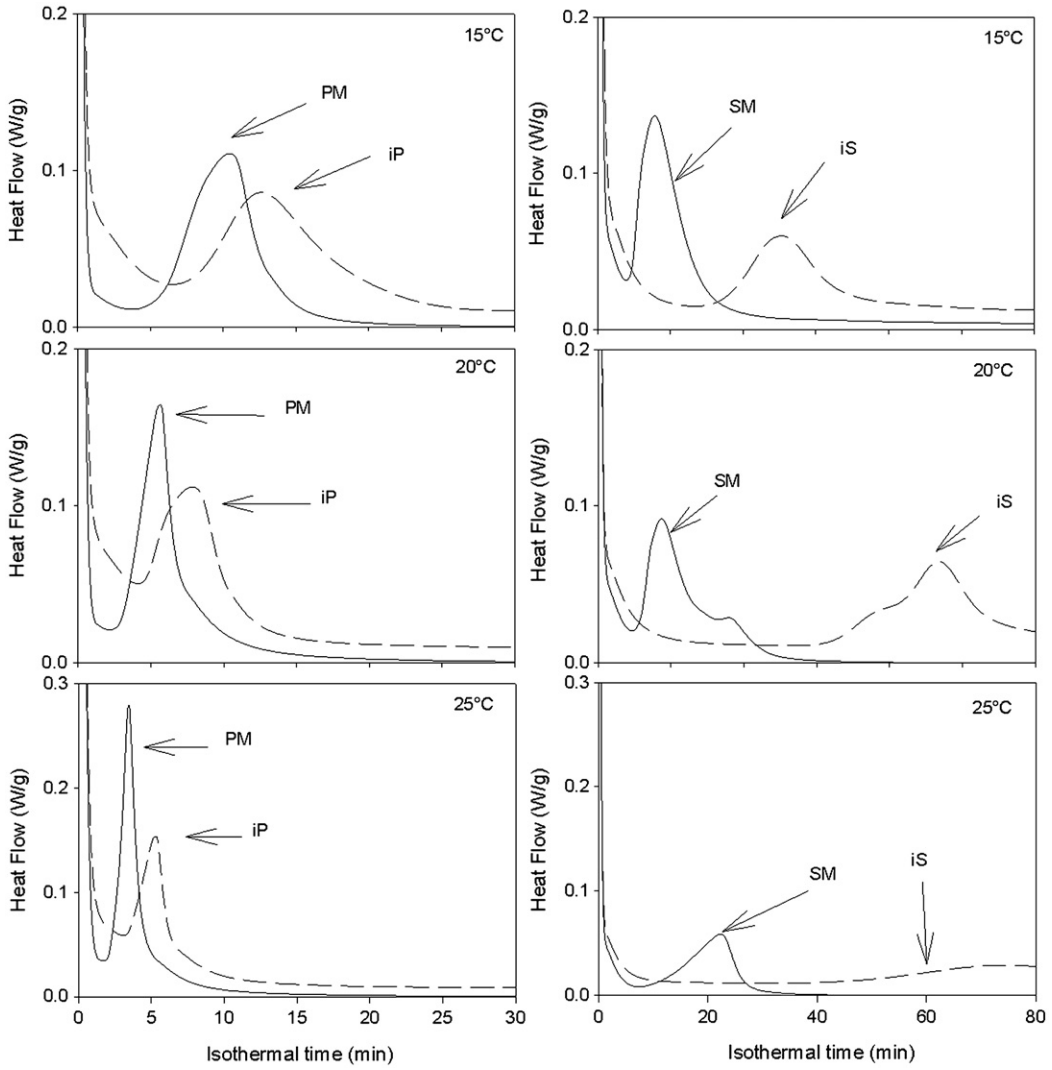

Fig. 3. Effect of TAG symmetry on the isothermal DSC profiles at 15 °C, 20 °C and 25 °C. Left side: palmitic based blends and right side: stearic based blends.

3.2.1. Palmitic based blends

The left side of Fig. 2 presents the isothermal crystallization of the palmitic based blends (blends PH, PM and PL) at 15, 20 and 25 °C. At all temperatures the same order of crystallization is observed. Blend PH (highest content of PPP) shows the highest crystallization rate, followed by blend PM and finally blend PL. The crystallization rate of blend PL at 20 °C and 25 °C is very slow, giving a crystallization profile that almost could not be discerned from the baseline. However, at higher temperatures, the crystallization peaks of blends PH and PM became smaller and shifted to lower isothermal times. This is unexpected because a higher crystallization temperature normally yields a slower crystallization and, consequently, a broader crystallization peak at later isothermal times, because of the decrease in driving force of crystallization (Himawan et al., 2006).

The left side of Fig. 4 displays the evolution of the melting enthalpy of the palmitic based blends at the three crystallization temperatures as obtained from the stop-and-return DSC experiments. The crystallization parameters obtained from fitting the Foubert (2003) model, are presented in Table 4.

The model parameter K [min^{-1}] is related to the crystallization rate as a faster crystallization is indicated by a higher value for this parameter. Indeed, blend PH has the highest value for this parameter at the three temperatures, followed by blend PM and then blend PL. The melting enthalpy at equilibrium, given by parameter a [J/g] of the Foubert (2003) model, is different for the different palmitic based blends. As for parameter K, blend PH has the highest value, followed by blend PM and then blend PL, which can be explained by the higher melting enthalpy of trisaturated TAG compared to disaturated and monosaturated TAG (Hagemann, 1988). From Fig. 4 it is also clear that the crystallization temperature is especially important for blend PL, leading to a decrease of the crystallization rate (lower value of the parameter K, see Table 4) and the amount of fat crystallized (lower value of the parameter a, see Table 4). Especially between 15 and 20 °C, there is a big reduction in the crystallization speed of the blend, which can also be observed in Fig. 2. At 25 °C, there is almost no crystallization for this blend. For blend PM, the crystallization temperature primarily influences the induction time of the second crystallization step which shortens for higher temperatures.

It can also be observed that, especially for blends PH and PM, the melting enthalpy is not zero at the start of the isothermal period, since crystallization has already begun during cooling. At higher temperatures the amount of fat crystallized during cooling decreases a little bit for blend PH, while its crystallization rate increases for higher temperatures as is expressed in the higher value of parameter K. Furthermore, Fig. 4 clearly indicates a two-step crystallization process for some of the blends, which can be due to either a polymorphic transition (e.g. α mediated β′ crystallization) or a fractionated crystallization (first a crystallization of a high melting fraction, then a crystallization of a low melting fraction). Finally, the parameter t_{ind} [min] gives an idea about the crystallization kinetics of the blends

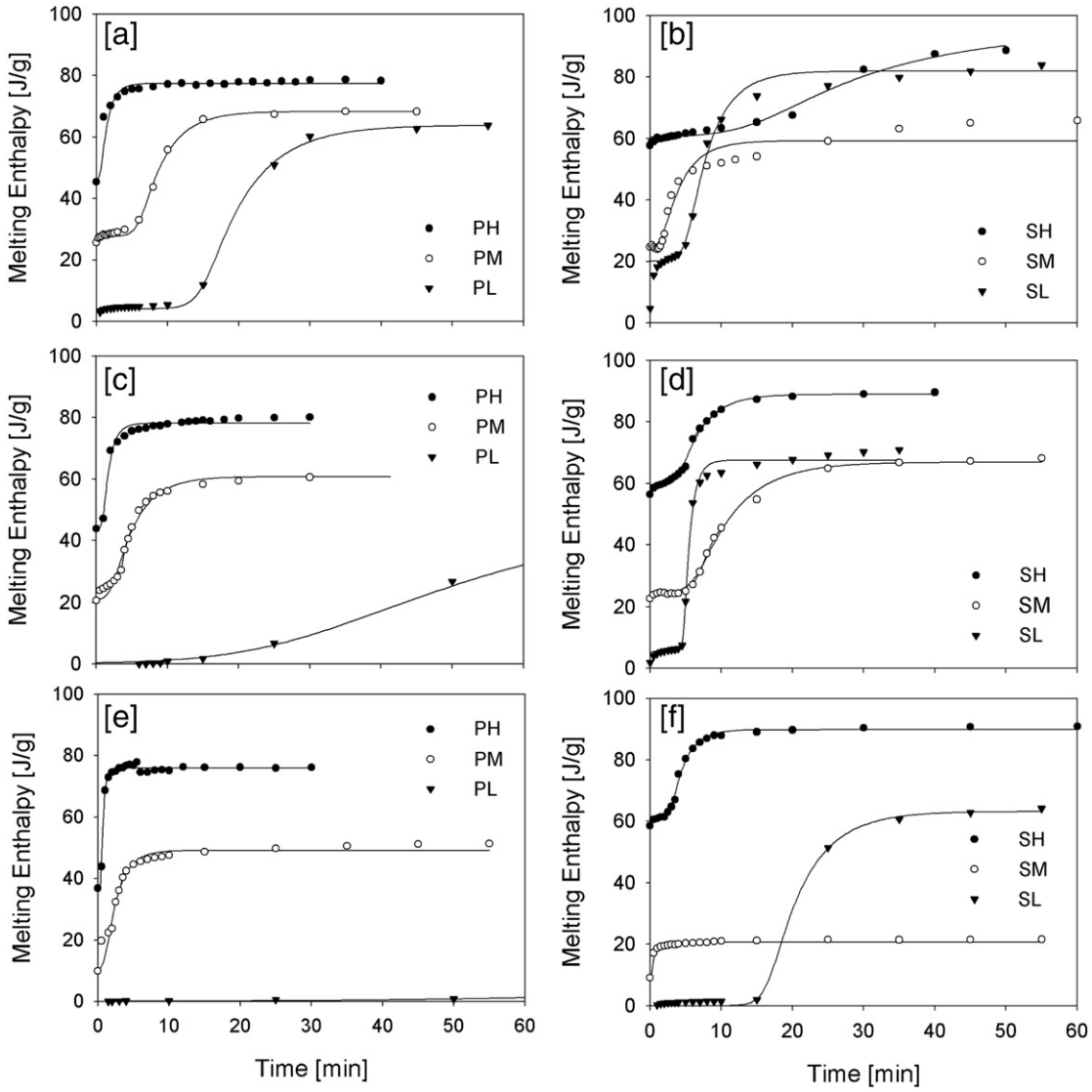

Fig. 4. Effect of trisaturated TAG on the DSC stop-and-return results for the different investigated blends: (a) palmitic based blends at 15 °C, (b) stearic based blends at 15 °C, (c) palmitic based blends at 20 °C, (d) stearic based blends at 20 °C, (e) palmitic based blends at 25 °C, and (f) stearic based blends at 25 °C. The solid lines give the fitting of the second crystallization stage to the Foubert (2003) model.

(Foubert, 2003). This parameter is especially low for blend PH (see Table 4), meaning that the second crystallization stage starts the earliest for this blend.

The pattern for the palmitic based blends PM and iP (see left side of Figs. 3 and 5) is the same for all three crystallization temperatures. Looking at the crystallization temperatures (see left side of Fig. 3), it is clear that the crystallization peaks of both blends shift to lower isothermal times (earlier crystallization) and become sharper (more instantaneous crystallization). As can be seen in Fig. 5 (left side), blend PM crystallizes faster than blend iP at the three temperatures. Both blends showed a quite fast two-step crystallization (fractional or polymorphic). At higher temperatures, the induction time and crystallization rate of the second crystallization step became shorter (Table 4).

3.2.2. Stearic based blends

In contrast to the palmitic based blends, the order of crystallization for the stearic based blends at 15 °C is completely different, as illustrated in Fig. 2 (right side) with the fastest crystallization for blend SL, followed by SM and SH. This can also be concluded from the values of parameter *K* (Table 4), obtained from the enthalpy curves presented in Fig. 4 (right side). At higher crystallization temperatures, the crystallization peak of blend SH shifts to earlier times and becomes sharper, while the peaks of blend SM and SL shift to later isothermal times and become broader. From Fig. 4 it can be concluded that for blend SH at all temperatures a significant amount crystallizes during the cooling period as the enthalpy is not zero at the beginning of the isothermal period. To a lesser extent this is also the case for SM, while for SL no crystallization takes place during the cooling period.

All blends show a two-step crystallization at 15 °C, which can be due to a polymorphic transition or fractionated crystallization. Furthermore, it is clear that, at 15 °C, the induction time of the second crystallization step is clearly shorter for blend SM compared to blend SL (see parameter t_{ind} in Table 4). At 20 °C, the induction time of the second crystallization step of blend SM increased compared to that at 15 °C. At 25 °C, no second crystallization step was observed for this blend within the observation time. At the three temperatures, this blend has quite a fast crystallization, which was especially the case at 20 °C (high value of the parameter *K*, see Table 4). At 15 °C and 20 °C, a two-step crystallization can be observed for blend SL, while at 25 °C the crystallization appears to be a single step process for this blend. On the other hand, the induction time of the second crystallization step of blend SH decreased clearly for higher crystallization temperatures (see Table 4 and right side of Fig. 4), which can be explained by an

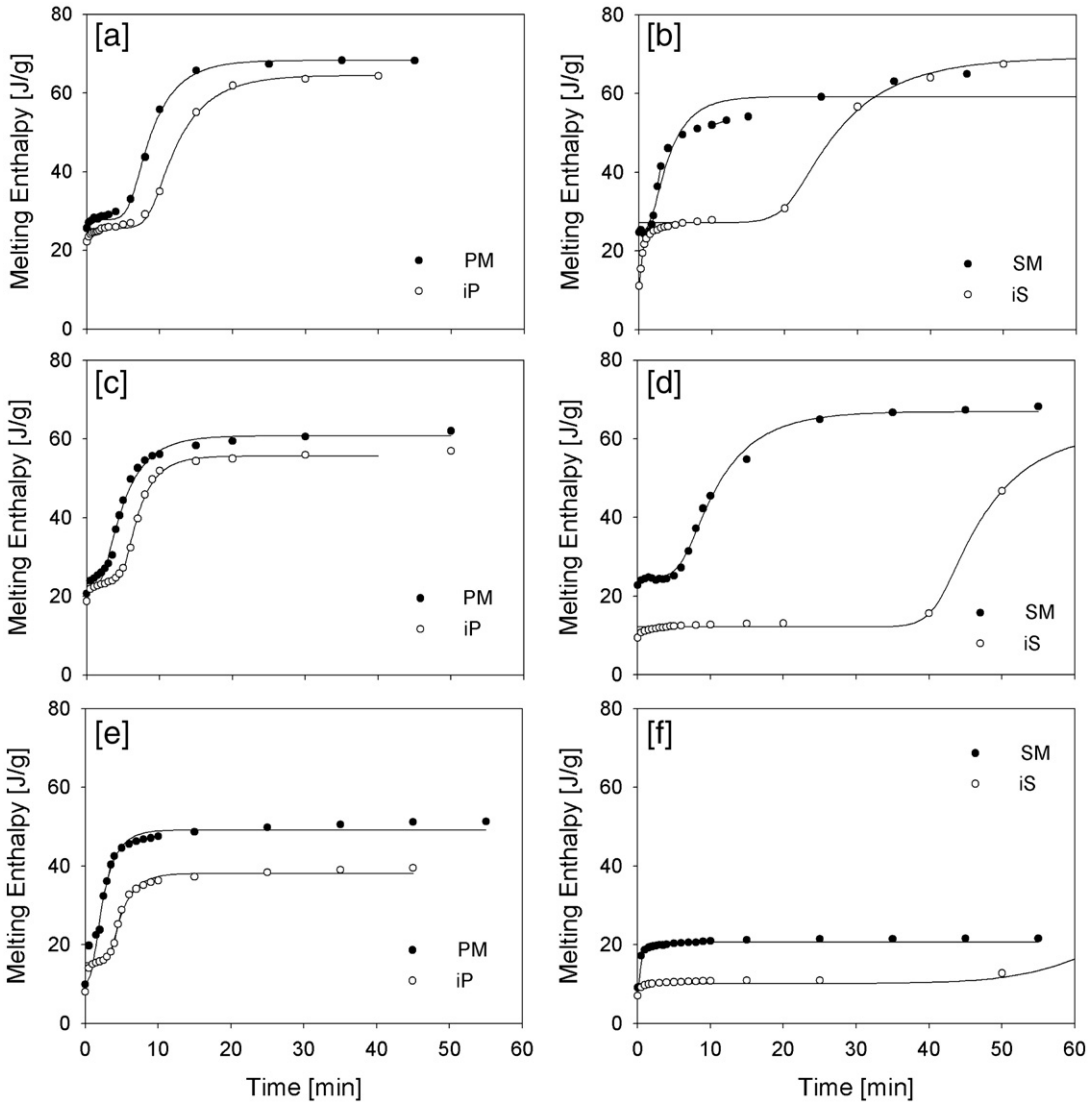

Fig. 5. Effect of TAG symmetry on the DSC stop-and-return results for the different investigated blends: (a) palmitic based blends at 15 °C, (b) stearic based blends at 15 °C, (c) palmitic based blends at 20 °C, (d) stearic based blends at 20 °C, (e) palmitic based blends at 25 °C, and (f) stearic based blends at 25 °C. The solid lines give the fitting of the second crystallization stage to the Foubert (2003) model.

increase of the rate of polymorphic transition at higher crystallization temperatures (Walstra, 1987).

In contrast to the palmitic based blends PM and iP, there appears to be a marked difference in the crystallization mechanism and/or crystallization kinetics of the two stearic based blends SM and iS (see right side of Figs. 3 and 5), especially at 20 °C and 25 °C. At 15 °C, the symmetric TAG based blend SM shows a clearly faster crystallization (higher value of *K* and shorter induction time, see Table 4) compared to the asymmetric TAG based blend iS. At higher temperatures, the difference in crystallization behaviour between both stearic-blends became larger, emphasizing the important role of the driving force of crystallization, especially for the interesterified blend iS. Not only the slope of the crystallization curve decreases (right side Fig. 5), but also the induction time of the second crystallization process increases. At 25 °C, no second crystallization step was observed at all for either blend during the 1 h of crystallization, illustrating the effect of crystallization temperature on the crystallization behaviour of both blends.

3.3. WAXD-analysis

As discussed in Section 3.2, most of the blends showed a two-step crystallization at the investigated temperatures, which could be explained either by polymorphism or by fractional crystallization (first a crystallization of a high melting fraction, then a crystallization of a low melting fraction). In a previous study of our group (Vereecken et al., 2009), the explanation of the mechanism of the two-step crystallization was obtained by looking at the peak maxima in the melting curves obtained from the stop-and-return experiments. Indeed, the peak maxima of the melting curves at different isothermal times will shift when there is a change of the polymorphic form or when there is fractional crystallization. A change of the polymorphic form is indicated by a shift of the peak maxima to higher temperatures as a function of the isothermal time due to the higher melting point of more stable polymorphs, while fractional crystallization would give a shift to lower temperatures due to the crystallization of a lower melting olein fraction after a higher melting stearin fraction.

Also, during this research the melting profiles obtained by stop-and-return were investigated to look at the shift in the peak maximum, but this did not lead to big differences. To give an example of the most common observed behaviour, Fig. 6 gives the evolution of the melting profile of blend SH at 20 °C for different isothermal times. At low isothermal times (start of the crystallization) both a low and a high melting peak were observed and also an exothermal peak was present around 55 °C (see Fig. 5). At longer isothermal times the low

Table 4
Model parameters of the Foubert (2003) model derived from the stop-and-return experiments presented in Figs. 4 and 5.

Blend	Temperature (°C)	a [J/g]	t_{ind} [min]	K [min^{-1}]	Adj. R^2
PH	15	77.38	0.00	0.96	0.984
	20	78.14	0.42	1.05	0.974
	25	75.88	0.26	2.97	0.993
PM	15	68.32	3.98	0.28	0.997
	20	60.77	0.37	0.31	0.986
	25	49.15	0.00	0.56	0.959
PL	15	63.83	11.32	0.16	0.999
	20	57.86	3.19	0.02	0.998
	25	15.17	12.19	0.01	0.998
iP	15	64.51	6.21	0.22	0.998
	20	55.63	3.69	0.41	0.998
	25	38.13	2.35	0.52	0.994
SH	15	95.25	3.69	0.05	0.985
	20	88.94	2.14	0.31	0.995
	25	89.79	1.75	0.51	0.995
SM	15	59.22	0.00	0.35	0.919
	20	66.89	3.08	0.18	0.996
	25	20.65	0.00	2.58	0.903
SL	15	81.89	3.13	0.29	0.993
	20	67.52	4.20	1.07	0.997
	25	63.19	13.62	0.20	0.998
iS	15	69.15	15.82	0.12	0.999
	20	62.28	36.81	0.13	0.999
	25	64.25	43.11	0.03	0.999

melting peak and exothermal peak disappeared and the high melting peak was the only remaining peak. Based on Vereecken et al. (2009), this behaviour might be explained by a polymorphic transition (as indicated in Fig. 6), but to be completely sure about this, X-ray diffraction is needed. Therefore, the blends were subjected to WAXD-analysis to derive the lateral packing of the fat crystals. For blends PH, PM, iP and SH no difference in crystallization behaviour was observed with DSC-analysis at the three temperatures investigated, so these blends were only analyzed at 20 °C.

The short spacings and the corresponding polymorphic forms for the different blends at the investigated temperatures are given in Table 5. For all the blends, except blend PL at 20 °C, a shift in the WAXD-pattern was observed, although not all the blends appeared to show a two-step crystallization when looking at the enthalpy curves (e.g. blend PH, see Fig. 4). This can be explained by the fact that a high amount of fat already crystallized during the cooling period and the transition to the second step happened at low isothermal times, making it difficult to observe the two-step crystallization.

The identification of the polymorphs, mentioned in Table 5, was based on literature data. An α polymorph is characterized by a strong spacing around 4.15 Å. A β′ polymorph is characterized by spacings around 3.8 and 4.2 Å, while a β polymorph is characterized by

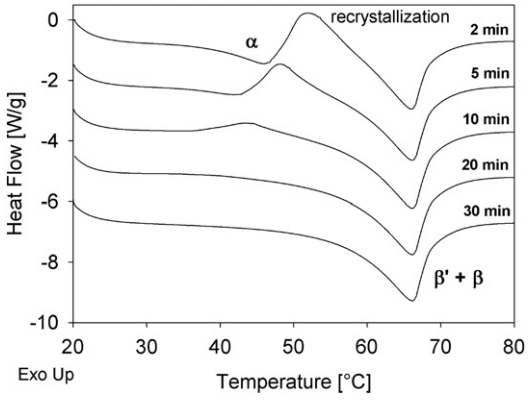

Fig. 6. Melting profiles after certain isothermal times during the stop-and-return analysis of blend SH at 20 °C.

Table 5
Short spacings and corresponding polymorphic forms, derived from WAXD-analysis, of the eight blends investigated.

Blend	T_{cr} (°C)	First step (Å)	Polymorph	Second step (Å)	Polymorph
PH	20	4.19 (vs)	α	3.82 (s), 3.95 (s), 4.63 (m)	B
PM	20	4.20 (vs)	α	3.92 (s), 4.07 (m), 4.24 (s), 4.60 (m)	β′≫β
PL	15	4.20 (s)	α	4.00 (s), 4.28 (s)	β′
	20	–	–	4.00 (s), 4.30 (s)	β′
iP	20	4.17 (vs)	α	3.90 (s), 4.21 (s), 4.35 (s)	β′
SH	20	4.17 (vs)	α	3.80 (s), 3.92 (s), 4.64 (m)	β
SM	15	4.16 (vs)	α	3.95 (m), 4.14 (s), 4.59 (m)	β′>β
	20	4.16 (vs)	α	3.90 (s), 4.16 (m), 4.37 (w), 4.57 (m)	β′>β
	25	4.16 (vs)	α	3.95 (m), 4.42 (w), 4.58 (m)	β′≈β
SL	15	4.13 (s)	α	3.64 (w), 3.86 (vs), 4.49 (m), 4.67 (s)	β≫β′
	20	4.16 (m)	α	3.86 (vs), 4, 14 (w), 4.49 (m), 4.68 (s)	β>β′
	25	4.17 (w)	α	3.88 (s), 4.13 (vs), 4.33 (s), 4.67 (w)	β′≫β
iS	15	4.17 (s)	α	3.9 (s), 4.18 (w), 4.72 (m)	β>β′
	20	4.20 (s)	α	3.88 (m), 4.2 (vs)	β′
	25	4.18 (s)	α	3.93 (w), 4.18 (s), 4.38 (m), 4.60 (w)	β′≫β

spacings between 3.7 and 3.9 Å and around 4.6 Å (Hagemann, 1988; Himawan et al., 2006). An example of the WAXD-pattern observed is given in Fig. 7, showing the WAXD-pattern of blend SH during the isothermal crystallization at 20 °C.

4. Discussion

4.1. Effect of trisaturated TAG

PPP seems to act as a seeding agent to increase the crystallization rate of the blends. More specifically, it seems that PPP promotes the crystallization of POP, which is especially seen by the fast crystallization kinetics of blend PM having a high level of both POP and PPP (see Table 3). Blend PL contains very low amounts of PPP, leading to a significantly lower crystallization rate, especially at higher crystallization temperatures (see left side of Figs. 2 and 4). Other studies have also shown that PPP can promote the crystallization rate of POP by specific interactions (Minato et al., 1996; Smith et al., 2005; Vereecken et al., 2009). The shorter induction time for the second crystallization step of blend PH and PM at higher temperatures can possibly be explained by a faster transition to more stable polymorphs at higher temperatures (Walstra, 1987). For blend PH, the effect of the crystallization temperature is limited, due to the high driving force at the three crystallization temperatures (effect of PPP).

On the other hand, the effect of trisaturated TAG is less clear for the stearic based blends (see Table 4 and right side of Figs. 2 and 4). From Fig. 4 it is clear that blend SH, which has a very high melting point due to the high amount of tristearin (see Table 3), crystallizes almost completely during the cooling period and consequently only a remaining slow crystallizing part will crystallize during the isothermal period. This gives an explanation for the lower observed crystallization rate compared to the other stearic based blends. An explanation for the lower crystallization rate of blend SM compared to blend SL, observed in Fig. 2 (15 °C), is that the different TAG in blend SM interact in a non-ideal way, e.g. without the formation of mixed crystals, giving a slower crystallization of the blend. For example, SSS may not act as a seeding agent for the other (mainly SOS) TAG in blend

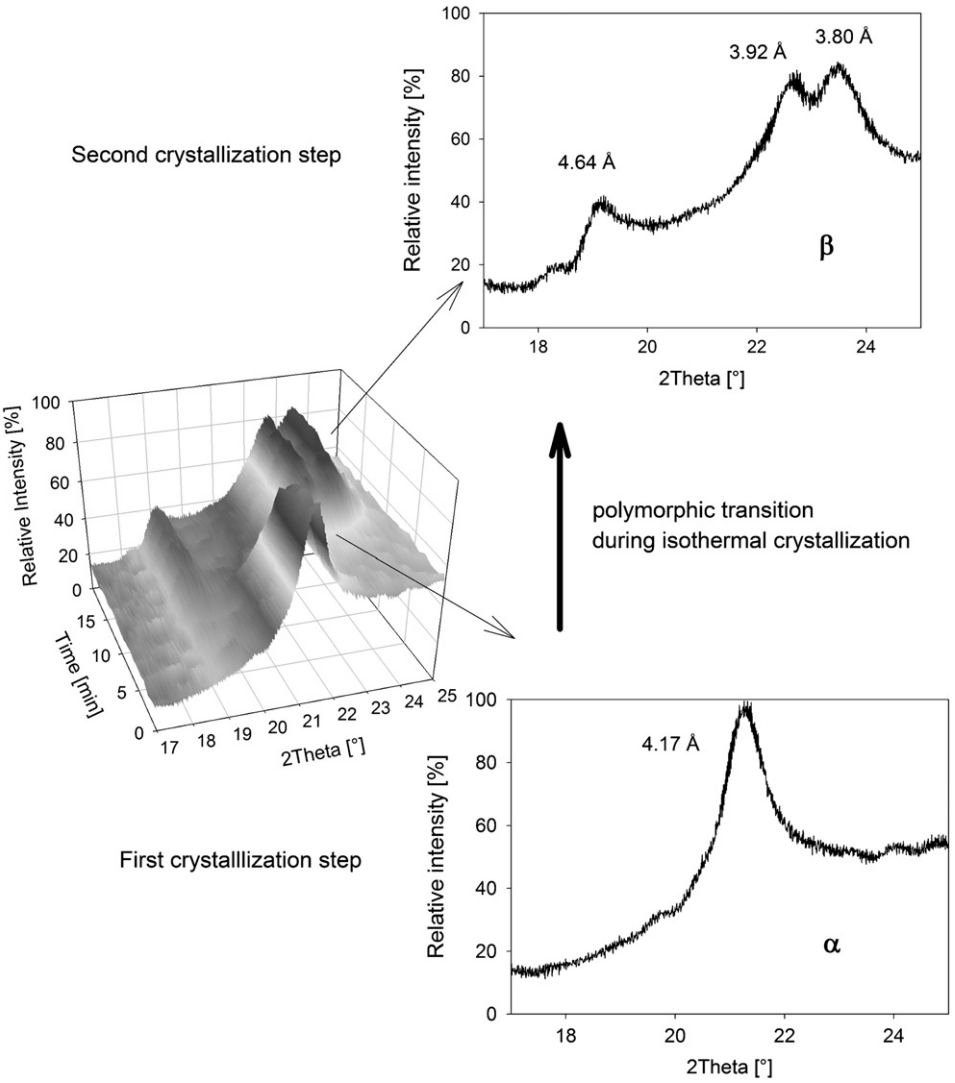

Fig. 7. WAXD-pattern during the isothermal crystallization of blend SH at 20 °C.

SM and may retard the crystallization of SOS in the blend (Vereecken et al., 2009). This suggests that SSS does not interact in the same way with SOS as PPP does with POP. The formation of mixed crystals between SSS and SOS did not favour the crystallization kinetics of blend SM.

On the other hand, the induction time for the second crystallization step at 15 °C is markedly shorter for blend SM than for blend SL, which can be explained by the higher amount of trisaturated TAG in blend SM. In contrast, the equilibrium melting enthalpy is higher for blend SL compared to blend SM, which may be explained by a different polymorphic behaviour or possible non-ideal phase behaviour occurring between the different TAG present in blend SM (Timms, 1984).

A higher crystallization temperature gave a different behaviour for the three stearic based blends presented in Figs. 2 and 4. The crystallization peak of blend SH shifted to earlier times (shorter induction time of the second crystallization step, see Table 4) and became sharper, which can be explained by the decrease in the amount of fat crystallized during cooling and the faster polymorphic transition at higher temperatures (Walstra, 1987). The crystallization of blend SM clearly slowed down at higher temperatures, due to the decrease in driving force of crystallization at higher temperatures (Himawan et al., 2006). For blend SL, the crystallization peak was quite sharp at 15 and 20 °C. When looking at the composition of this blend (see Table 3), it is clear that this blend contains a quite high amount of a single TAG group, namely SatOSat, which is an explanation for the fast crystallization and the sharp crystallization peaks. It is thus clear that the crystallization temperature can have a completely different effect on the crystallization of the blends, especially in the case of the stearic based blends in this research.

4.2. Effect of symmetry

For the palmitic based blends, blend PM shows a faster crystallization at the three temperatures compared to blend iP, which might be explained by the slightly lower melting point of PPO and of the POP/PPO compound present in blend iP. Indeed, Engstrom (1992) mentions that the melting point of the most stable form of POP is 36.6 °C, the melting point of PPO is 34.6 °C and the melting point of the compound POP/PPO is 31.2 °C. This compound is formed at a 1:1-concentration of POP and POP, so, when looking at Table 3, PPO will probably be present both alone and in a molecular compound with POP/PPO (excess amount of PPO) in blend iP. Although there are some differences for the palmitic based blends, it might be concluded that these differences are quite small and both blends possess a comparable crystallization behaviour. It could be that the two blends show a different polymorphic behaviour, since it is well-known that symmetric and asymmetric TAG pack in totally different ways. For example, the most stable form of POP is the β-polymorph, while the

most stable form of PPO is the β′-polymorph (Minato et al., 1997). This will further be discussed in Section 4.3.

When looking at the stearic based blends SM and iS, a broad crystallization peak was observed for blend iS (Fig. 3), especially at 20 and 25 °C, which may be due to the broader TAG composition of the interesterified TAG blend iS, as shown in Table 3. Another explanation is the sequential crystallization of different polymorphic forms. Or perhaps, the presence of such a broad composition simply slows crystallization due to the increased time required for molecular sorting to occur at the solid–liquid interface. Many different crystal types could be formed in blend iS, for example, the formation of the compound crystal SOS/SSO. Following Takeuchi et al. (2002), this compound forms, just like for the POP/PPO compound, at a 1:1 ratio of SOS and SSO. The slower crystallization behaviour of the asymmetric based blend can be explained by the broader TAG composition of this blend (see also above) and by the lower melting point of asymmetric TAG compared to symmetric TAG (Takeuchi et al., 2002).

4.3. Effect of chain length

The effect of chain length can be evaluated by comparing the left side with the right side in Figs. 2–5. Blends PH, PM and iP seem to show a faster crystallization than their stearic based counterparts, which may be explained by the better packing of the different TAG in these blends. Indeed, mixed crystals and compound crystals with palmitic based TAG are clearly described in literature (Minato, Ueno, Yano et al., 1996; Minato, Ueno, Smith et al., 1997; Smith et al., 2005; Himawan et al., 2006).

On the other hand, blend PL clearly crystallizes slower than blend SL, especially at higher temperatures. This might be explained by the lower melting point of POP (36.6 °C) compared to SOS (43.8 °C) (Engstrom, 1992), leading to a lower driving force for crystallization.

4.4. Polymorphic behaviour of the blends

As shown in Fig. 6 and described in Section 3.3, the evolution of the peak maxima during the stop-and-return experiments suggested the presence of a polymorphic transition during the isothermal crystallization with a transition from an unstable polymorph (possible an α polymorph) to a more stable polymorph (possibly a β′ or β polymorph). The same type of behaviour was also observed during the isothermal crystallization of palm oil, as investigated by Chen, Lai, Ghazali, and Chong (2002).

WAXD was used to further identify the polymorphic behaviour of the blends and to prove the above-mentioned hypothesis. From Table 5 it is clear that all the blends, except blend PL at 20 °C, indeed crystallize firstly into an α polymorph and subsequently undergo a polymorphic transition to a β′ or β (or a mixture of a β′ and β) polymorph. In contrast, no β polymorph was found for blend PL at all the crystallization temperatures (the low amount of fat crystallized for blend PL at 25 °C (see Fig. 4) gave a diffraction pattern which was too weak to be analyzed). Only the β′ polymorph was observed (see Table 5). Possibly, the driving force for crystallization of this blend is too low to give a transition to the stable β polymorph.

For blend iP, only the β′ polymorph was observed, which can be explained by the β′ stability of asymmetric TAG (Timms, 2003). For blend iS, also the β polymorph was observed, especially at 15 °C crystallization (see Table 5). This can possibly be explained by the β-stability of the compound SOS/SSO (S = stearic acid), formed at 1:1 concentration (Takeuchi et al., 2002), which may be present in the blend (see Table 3).

The occurrence of the β′ or β polymorph is dependent on the TAG composition of the blends, as given in Table 3. Trisaturated TAG (SatSatSat, Sat = saturated) and symmetric TAG (SatOSat) are known easily to form a β polymorph, which is the most stable polymorph of these TAG (Timms, 2003). This is the explanation for the observed β-polymorph in blends PH and SH. Because of their high melting point, the driving force of these blends is high enough to give a fast transformation of their fat crystals to the most stable polymorph. However, when a lot of other TAG are present (increased heterogeneity), fat systems are more likely to form β′ stable crystals or mixtures of β′ and β crystals (Timms, 2003; Piska, Zarubova, Louzeka, Karami, & Filip, 2006). This is the explanation for the β′ stability of palm oil, although this oil contains a high amount of the β stable TAG POP (Timms, 2003). This explains the mixture of the β′ and β polymorphs found for blends PM, SM and SL.

5. Conclusions

In this study, the crystallization of eight blends containing the same amount of saturated fatty acids (50%), but having a different TAG composition, was investigated and compared by DSC and XRD (WAXD). Three different effects were investigated, namely the effect of the amount of trisaturated TAG, the effect of symmetry and the effect of chain length.

Aside from the anticipated effects (i.e. greater levels of SatSatSat lead to faster crystallization), isothermal DSC, using the stop-and-return method, showed that PPP had a greater influence on the crystallization of POP than did SSS on SOS. Moreover, the effect of symmetry was more pronounced for the stearic based TAG compared to the palmitic based TAG. This can possibly be explained by the better compound (e.g. POP–PPO) and mixed crystal formation in the palmitic based blends compared to the stearic based blends.

WAXD-analyses of the samples revealed that the two-step crystallization, observed during the DSC-stop and return experiments, could be explained by a polymorphic transition of the unstable α polymorph to the more stable β′ and β polymorphs. The occurrence of the β′ or β polymorph varied between blends, which can be explained by their different TAG compositions.

The results demonstrate the importance of formulating the TAG composition of a fat in order to achieve the desired crystallization properties and the formation of the desired polymorphic form. This can be extremely important for the further structure development in the fats and fat rich products, as also explained by Narine and Marangoni (1999).

Acknowledgements

We are grateful to Dessy Natalia for performing the experimental part of the research and we thank Loders Croklaan for the financial support and for providing the fat samples. Gary Sassano (Unilever Research Colworth) is acknowledged for carrying out the TAG analysis. Bernadette Norberg is acknowledged for the help with the WAXD-analyses at the University of Namur.

References

Braipson-Danthine, S., & Gibon, V. (2007). Comparative analysis of triacylglycerol composition, melting properties and polymorphic behavior of palm oil and fractions. *European Journal of Lipid Science and Technology*, *109*(4), 359−372.

Chen, C. W., Lai, O. M., Ghazali, H. M., & Chong, C. L. (2002). Isothermal crystallization kinetics of refined palm oil.*Journal of the American Oil Chemists' Society*, *79*(4), 403 410.

Danthine, S., & Deroanne, C. (2003). Physical and textural characteristics of hydrogenated low-erucic acid rapeseed oil and low-erucic acid rapeseed oil blends. *Journal of the American Oil Chemists' Society*, *80*(2), 109−114.

Deffense, E. (1985). Fractionation of palm oil. *Journal of the American Oil Chemists' Society*, *62*(2), 376−385.

Engstrom, L. (1992). Triglyceride systems forming molecular compounds. *Journal of Fat Science and Technology*, *94*(5), 173−181.

Foubert, I. (2003). Modelling isothermal cocoa butter crystallization: Influence of temperature and chemical composition, PhD Thesis, Ghent University, Ghent (Belgium).

Foubert, I., Fredrick, E., Vereecken, J., Sichien, M., & Dewettinck, K. (2008). Stop-and-return DSC method to study fat crystallization. *Thermochimica Acta*, *471*(1–2), 7−13.

Foubert, I., Vanrolleghem, P., & Dewettinck, K. (2003). A differential scanning calorimetry method to determine the isothermal crystallization kinetics of cocoa butter. *Thermochimica Acta*, *400*, 131—142.

Hagemann, J. W. (1988). Thermal behaviour and polymorphism of acylglycerides. In N. Garti, & K. Sato (Eds.), *Crystallization and polymorphism of fats and fatty acids* (pp. 9—95). New York: Marcel Dekker Inc.

Himawan, C., Starov, V. M., & Stapley, A. G. F. (2006). Thermodynamic and kinetic aspects of fat crystallization. *Advances in Colloid and Interface Science*, *122*(1–3), 3—33.

Jeffrey, B. S. (1991). Silver-complexation liquid chromatography for fast, high-resolution separation of triacylglycerols. *Journal of the American Oil Chemists' Society*, *68*(5), 289—293.

Karabulut, I., Turan, S., & Ergin, G. (2004). Effects of chemical interesterification on solid fat content and slip melting point of fat/oil blends. *European Food Research and Technology*, *218*(3), 224—229.

List, G. R. (2004). Decreasing trans and saturated fatty acid content in food oils. *Food Technology*, *58*(1), 23—31.

Marangoni, A. G. (2002). Special issue of FRI — Crystallization, structure and functionality of fats. *Food Research International*, *35*(10), 907—908.

Minato, A., Ueno, S., Smith, K., Amemiya, Y., & Sato, K. (1997). Thermodynamic and kinetic study on phase behavior of binary mixtures of POP and PPO forming molecular compound systems. *Journal of Physical Chemistry B*, *101*(18), 3498—3505.

Minato, A., Ueno, S., Yano, J., Wang, Z. H., Seto, H., Amemiya, Y., et al. (1996). Synchrotron radiation X-ray diffraction study on phase behaviour of PPP–POP binary mixtures. *Journal of the American Oil Chemists' Society*, *73*(10), 1567—1572.

Narine, S. S., & Marangoni, A. G. (1999). Relating structure of fat crystal networks to mechanical properties: A review. *Food Research International*, *32*(4), 227—248.

Piska, I., Zarubova, M., Louzeka, T., Karami, H., & Filip, V. (2006). Properties and crystallization of fat blends. *Journal of Food Engineering*, *77*, 433—438.

Sato, K. (2001). Crystallization behaviour of fats and lipids — A review. *Chemical Engineering Science*, *56*(7), 2255—2265.

Smith, K. W., Cain, F. W., & Talbot, G. (2005). Crystallization of 1,3-dipalmitoyl-2-oleoylglycerol and tripalmitoylglycerol and their mixtures from acetone. *European Journal of Lipid Science and Technology*, *107*(9), 583—593.

Takeuchi, M., Ueno, S., & Sato, K. (2002). Crystallization kinetics of polymorphic forms of a molecular compound constructed by SOS (1,3-distearoyl-2-oleoyl-sn-glycerol) and SSO (1,2-distearoyl-3-oleoyl-rac-glycerol). *Food Research International*, *35*(10), 919—926.

Timms, R. E. (1984). Phase behavior of fats and their mixtures. *Progress in Lipid Research*, *23*(1), 1—38.

Timms, R. E. (2003). *Confectionery fats handbook — Properties, production and application.*Bridgewater: The Oily Press 441 pp.

Toro-Vazquez, J. F., Briceno-Montelongo, M., Dibildox-Alvarado, E., Charo-Alonso, M., & Reyes-Hernandez, J. (2000). Crystallization kinetics of palm stearin in blends with sesame seed oil. *Journal of the American Oil Chemists' Society*, *77*(3), 297—310.

Vereecken, J., Foubert, I., Smith, K. W., & Dewettinck, K. (2009). Effect of SatSatSat and SatOSat on crystallization of model fat blends. *European Journal of Lipid Science and Technology*, *111*(3), 243—258.

Vereecken, J., Foubert, I., Smith, K. W., & Dewettinck, K. (2010). Crystallization of model fat blends containing symmetric and asymmetric monounsaturated triacylglycerols. *European Journal of Lipid Science and Technology*, *112*(3), 233—245.

Walstra, P. (1987). Fat crystallization. In V. M. V. Blanshard, & P. Lillford (Eds.), *Food structure and behaviour* (pp. 67—85). London: Academic Press.

Wesdorp, L. H. (1990). Liquid-multiple solid phase equilibria in fats — Theory and experiments. PhD Thesis, Technische Universiteit Delft, Delft (The Netherlands).

Zaliha, O., Chong, C. L., Cheow, C. S., Norizzah, A. R., & Kellens, M. J. (2004). Crystallization properties of palm oil by dry fractionation. *Food Chemistry*, *86*(2), 245—250.

Zhang, H., Smith, P., & Adler-Nissen, J. (2004). Effects of degree of enzymatic interesterification on the physical properties of margarine fats: Solid fat content, crystallization behavior, crystal morphology and crystal network. *Journal of Agricultural and Food Chemistry*, *52*(14), 4423—4431.